

FIG. 10. The global z magnetization of the spin chain of length $L = 13$ starting in a fully polarized state subjected to different driving schemes. We show the exact stroboscopic dynamics of the chain at even period numbers with and without a metronome spin at the central site as well as the average Hamiltonian given in Eq. (5). The configurations that include a metronome spin display lifetime enhancements by several orders of magnitude. All data are well described through numerical cosine fits. On the second axis (in purple font) we display the single-spin magnetization of the metronome spin itself. The dephasing of the magnetization of the metronome coincides with the dephasing of the plateau.

again, leading to the intermediate plateau before the late-time Rabi oscillations.

APPENDIX C: NNN INTERACTIONS

Here we want to study a modified version of the original interaction Hamiltonian H_{int} given in Eq. (1). We include additional next-to-nearest-neighbor (NNN) interactions to the model,

$$H_{\text{int}}^{\text{NNN}} = H_{\text{int}} + \sum_{i=1}^{L-2} J_{i,i+2} s_z^i s_z^{i+2}, \quad (\text{C1})$$

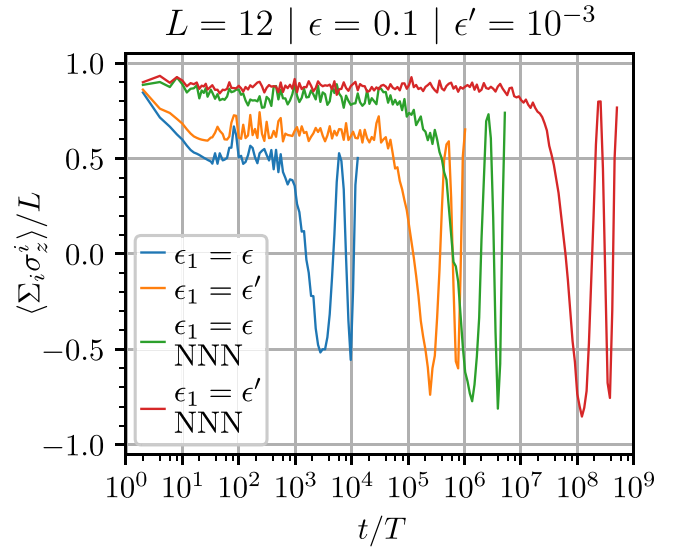


FIG. 11. The global z magnetization of the spin chain of length $L = 12$ starting in a fully polarized state subjected to different interaction Hamiltonians. We show the exact stroboscopic dynamics of the chain at even period numbers with and without a metronome spin at one boundary site, for both the standard and the integrability-breaking model (denoted NNN). Configurations that include a metronome spin display a lifetime enhancement of several orders of magnitude. For better visibility, only the first two oscillation cycles are plotted for each curve.

which break the integrability of the new effective Floquet Hamiltonian. We study the global magnetization of a polarized initial state of $L = 12$ spins subjected to the modified Floquet sequence with $H_{\text{int}}^{\text{NNN}}$ replacing the original interaction Hamiltonian H_{int} . We give the results for $J_{i,i+2} = 0.6$ and $\epsilon' = 10^{-3}$ in Fig. 11.

Both the standard model evolved through H_{int} (blue and orange curves) and the modified model evolved through $H_{\text{int}}^{\text{NNN}}$ (green and red curves) experience qualitatively comparable lifetime enhancements $\sim 1/\epsilon'$ through the addition of a metronome spin.

- [1] F. Wilczek, Quantum time crystals, *Phys. Rev. Lett.* **109**, 160401 (2012).
- [2] A. Shapere and F. Wilczek, Classical time crystals, *Phys. Rev. Lett.* **109**, 160402 (2012).
- [3] H. Watanabe and M. Oshikawa, Absence of quantum time crystals, *Phys. Rev. Lett.* **114**, 251603 (2015).
- [4] While Ref. [3] proved the impossibility of time crystals in equilibrium states of short-range interacting systems, a recent work observed stable time-periodic oscillations in the ground state of a system at equilibrium with long-range multispin interactions [56].
- [5] D. V. Else, B. Bauer, and C. Nayak, Floquet time crystals, *Phys. Rev. Lett.* **117**, 090402 (2016).
- [6] D. V. Else, C. Monroe, C. Nayak, and N. Y. Yao, Discrete time crystals, *Annu. Rev. Condens. Matter Phys.* **11**, 467 (2020).
- [7] K. Sacha, Modeling spontaneous breaking of time-translation symmetry, *Phys. Rev. A* **91**, 033617 (2015).
- [8] V. Khemani, R. Moessner, and S. L. Sondhi, A brief history of time crystals, arXiv:1910.10745.
- [9] D. A. Abanin, W. D. Roeck, and F. Huveneers, Theory of many-body localization in periodically driven systems, *Ann. Phys. (NY)* **372**, 1 (2016).
- [10] V. Khemani, A. Lazarides, R. Moessner, and S. L. Sondhi, Phase structure of driven quantum systems, *Phys. Rev. Lett.* **116**, 250401 (2016).
- [11] N. Y. Yao, A. C. Potter, I.-D. Potirniche, and A. Vishwanath, Discrete time crystals: Rigidity, criticality, and realizations, *Phys. Rev. Lett.* **118**, 030401 (2017).
- [12] H. Burau, M. Heyl, and G. De Tomasi, Fate of algebraic many-body localization under driving, *Phys. Rev. B* **104**, 224201 (2021).